Eur. Phys. J. D **41**, 9–23 (2007)
DOI: 10.1140/epjd/e2006-00185-0

THE EUROPEAN PHYSICAL JOURNAL D

Weak and strong coupling regimes, vacuum Rabi splitting and two types of resonances

C. Billionnet[a]

Centre de Physique Théorique, École Polytechnique, 91128 Palaiseau Cedex, France

Received 4 January 2006 / Received in final form 6 June 2006
Published online 5 August 2006 –

Abstract. For two discrete-level quantum systems in interaction, we follow the displacement in the complex plane of the eigen-energies of the compound system when the excited level of one of the two systems is enlarged. These new points are usually called resonances and describe mixed unstable states. This allows us to define and to calculate a critical value of the coupling constant which separates two well-known coupling regimes. These two regimes are thus described in a unified way. In the study, resonances which are usually not taken into account occur. They are studied in the large continuum case provided by the coupling of the hydrogen atom to the states of the transverse electromagnetic field in the vacuum. We justify that some of these resonances be neglected in this case.

PACS. 42.50.-p Quantum optics – 71.36.+c Polaritons – 73.21.-b Electron states and collective excitations in multilayers, quantum wells, mesoscopic, and nanoscale systems

1 Introduction

In this work, we are interested in states in which a discrete-level quantum system $\mathcal{S}$ is coupled to a continuum $\mathcal{C}$. The total system may be an atom coupled to the transverse electromagnetic field, in the vacuum or in a non perfect cavity, an electron in a quantum dot coupled to optical phonons or photons, an exciton coupled to optical phonons or photons in a microcavity. The continuum may also consist of electronic states, whereas $\mathcal{S}$ is a fixed energy photon.

Three points usually appear in the study of this question. The first one is the vacuum Rabi splitting, the fact that for a two level atom, for instance, the coupling of the atom to photons which are resonant with the transition splits the excited level. This is a simple fact of Quantum Mechanics (see for instance [1], p. 408). The second point is the distinction between the weak and strong coupling regimes of the interaction of $\mathcal{S}$ and $\mathcal{C}$. The third one is the existence of bound states or almost bound states of the $\mathcal{S}+\mathcal{C}$ system which occur at large coupling constant. We are going to show that these three points can be linked by the study of the resonances of the $\mathcal{S}+\mathcal{C}$ Hamiltonian in the complex plane.

Many experimental studies have been performed in recent years as regards the second point, in the various domains we mentioned in the first paragraph. It is not possible to quote them all. Some of them are specially related to the transition between the two regimes. Let us mention for instance [2], where mixed electron-phonon states in a quantum dot [3] are studied, or [4–7] and [8–11], about excitons coupled to phonons or photons, or also [12] in which the continuum is made of electronic states. Atoms in cavities are studied for instance in [13–17]. The resonances of the $\mathcal{S}+\mathcal{C}$ system are numerous, as we showed it in [18,19]. One often only considers the following two extreme situations. Either the imaginary parts of these resonances are practically zero (very narrow continuum) and the resonances are very close to eigenvalues, thus easily identifiable, or some imaginary parts are very large, and the corresponding resonances are either not known, or deliberately ignored. The interest which has been taken recently in intermediate situations, such as those which occur in solid state physics for some electron-phonon couplings, leads to take all these resonances into account, without limiting oneself to perturbative calculations.

In these intermediate situations, the coupling constant and the continuum's width have various values. The continuum's width actually depends on the states of $\mathcal{S}$. As regards the interaction of an atom with the transverse electromagnetic field, the coupling constant in the interaction Hamiltonian is indeed the fine structure constant, but the details of the effective coupling, its dependence with respect to the energy of the photon emitted in some transition, depends on the transition which is considered. For instance, in general, the spatial extension of the atom's states is a factor which affects the width of the continuum as it is seen by the atom. The larger the spatial extension, the narrower the continuum's shape and the closer to the reals the resonances. This influence of the spatial extension may be very important [20]. We shall use the coupling

[a] e-mail: billionnet@cpht.polytechnique.fr

to the photon of the hydrogen atom Rydberg states to measure this influence again and also to prepare possible later studies of large molecules or studies in strong interactions. Indeed, in the hydrogen atom case, we will show that only resonances perturbed from the free atom's energies are of interest, although states with principal quantum number n extend over a distance proportional to n. The reason is that wavelengths of transitions between two states are too large with respect to the mean extension of these states for the other resonances to play any role. It is nevertheless a fact that these other resonances exist and, to be concrete, we will calculate some of them.

In Section 2, we first introduce the question in a general and qualitative way. Then, through a two level model, we study the behaviour of the resonances under the variation of three parameters: the coupling constant, the continuum's width and a continuum/system detuning. This will lead us to a precise definition of a transition point between the strong and weak coupling regimes. We will meet the vacuum Rabi splitting (VRS) in the narrow continuum limit (a case of strong coupling regime). In Section 3, we will apply the general preceding analysis to several situations among those mentioned in the beginning of this introduction. Section 4 is devoted to the hydrogen atom.

2 General study of a discrete-level system coupled to a continuum

It is now clear that for any discrete-level system $\mathcal{S}$ coupled to a massless field, or more generally to a continuum, the number of eigenvalues or resonances of the Hamiltonian is much greater than the number of levels of $\mathcal{S}$. The term resonances here means poles of matrix elements of the Hamiltonian's resolvent. Even with photons having only one possible state, if their number is not limited, the number of these eigenvalues or resonances is already infinite. Now, the number of linearly independent possible states for each photon may be infinite and the number of discrete levels is itself infinite. This make three reasons why the Hamiltonian operates in an infinite dimensional space. In the case where $\mathcal{S}$ is coupled to a massless field, let us denote the Hilbert space of $\mathcal{S}$ by $\mathcal{H}_S$ and that of the field by $\mathcal{H}_{\rm rad}$. In a N-dimensional space, a hermitian matrix has N real eigenvalues (possibly degenerated). In [19], we showed that the number of resonances is comparable to the dimension of the states of the total system $\mathcal{S}+$ field rather than to the number of discrete $\mathcal{S}$-states. Since these two numbers are infinite, (more precisely card ($I\!N$)), we have to make this statement more precise: for any restriction of the Hamiltonian to finite-dimensional subspaces of $\mathcal{H}_{\mathcal{S}} \otimes \mathcal{H}_{\rm rad}$, the number (with degeneracies taken into account) of resonances of the restricted Hamiltonian is at least the dimension of these subspaces. (This dimension is not necessarily the product of the dimension of a subspace of $\mathcal{H}_{\mathcal{S}}$ by the dimension of a subspace of $\mathcal{H}_{\rm rad}$.) This is a somewhat important departure from the traditional small coupling description, if the continuum's width is neither zero nor large.

2.1 Two types of resonances

When the continuum's width is large, some of these resonances are the familiar ones which appear through the perturbative approach to the coupling: they are the energies of the $\mathcal{S}$-levels moved into the complex plane by the coupling. We call them $\mathcal{R}$-type resonances, according to the general following definition.

> ***Definition 1****: in the coupling of a discrete-level system $\mathcal{S}$ to a continuum $\mathcal{C}$, $\mathcal{R}$-type resonances (or eigenvalues) are resonances (or eigenvalues) which tend to the energies of eigenstates of $\mathcal{S}$, when the coupling constant λ tends to 0, the Hamiltonian being of the form λV. We call resonances (or eigenvalues) which do not have this property $\mathcal{C}$-type resonances (or eigenvalues).*

$\mathcal{R}$ and $\mathcal{C}$-types were respectively called 'standard' and 'nonstandard' in [18–21].

Let us note that $\mathcal{S}$ and $\mathcal{C}$ do not play a symmetrical role in this labelling. Let us also note that $\mathcal{S}$ may be a material system and the continuum the set of states of the radiation. But it may be the other way round (see Sect. 3.2). We refer to the next to last paragraph of Section 2.3 for a justification of distinguishing two types of resonances.

Of course, the study of these resonances requires that a Hamiltonian be given, but we will begin with general considerations, without specifying the interaction. In the whole Section 2, the continuum is that of the states of a free scalar photon.

2.2 Coupling functions

Let us denote the eigenstates of $\mathcal{S}$ by $|0\rangle, |1\rangle, ...$ and set

$$H = \sum_n E_n |n\rangle\langle n| \otimes 1 + 1 \otimes H_{\rm rad} + H_I \qquad (1)$$

the Hamiltonian of the $\mathcal{S} + field$ system. $H_{\rm rad}$ is the Hamiltonian of the free field. Let us assume that for all $n > m$ and all $\varphi \in \mathcal{F}_1$, the one-photon-state space, there are functions g_{nm} such that

$$\langle n|H_I|m;\varphi\rangle = \int \varphi(k) g_{nm}(k) dk \qquad (2)$$

(we set $|m;\varphi\rangle = |m\rangle \otimes \varphi$). Thus, formally, we have

$$g_{nm}(k) = \langle n|H_I|m;k\rangle \qquad (2')$$

and $g_{nm}(k)$ describes the coupling of state $|m\rangle$ to state $|n\rangle$ through absorption of a photon with wave-vector k. We call $||g_{nm}||_2^{-1} g_{nm}$ the coupling function. ($||g_{nm}||_2$, the L^2-norm, has the dimension of an energy.) Generally, H_I has a lot of other a priori non-zero matrix elements than (2). We consider the following approximation of H

$$H^{\rm app} := \sum_n E_n |n\rangle\langle n| \otimes 1 + 1 \otimes H_{\rm rad} + H_I^{\rm app} \qquad (3)$$

with

$$H_I^{\rm app} := \sum_{m<n} \Big(|n\rangle\langle m| \otimes a(g_{nm}) + |m\rangle\langle n| \otimes \big(a(g_{nm})\big)^* \Big) \qquad (3')$$

where $a(.)$ is the field's annihilation operator : $a(g_{nm}) = \int a_k g_{nm}(k)dk$. This Hamiltonian neglects matrix elements of H_I between states the number of photons of which differs by more than one, as well as matrix elements $\langle m|H_I|n;k\rangle$ with $m < n$.

2.3 An example of a couple of a $\mathcal{R}$-type and a $\mathcal{C}$-type resonance: the vacuum Rabi splitting

$\mathcal{C}$-type resonances are easily seen in the limit where each g_{nm} is replaced by a delta function at point k_{nm}. (They become $\mathcal{C}$-type eigenvalues.) Let us show this. The interaction Hamiltonian (3) becomes

$$H_I^{\rm dis} := \sum_{m<n} \lambda_{nm}\Big(|n\rangle\langle m| \otimes a_{k_{nm}} + |m\rangle\langle n| \otimes a^*_{k_{nm}}\Big). \quad (4)$$

Let us set

$$H^{\rm dis} := \sum_n E_n|n\rangle\langle n| \otimes 1 + 1 \otimes \sum_{m<n} \hbar c k_{nm} a^*_{k_{nm}} a_{k_{nm}} + H_I^{\rm dis}. \quad (5)$$

Eigenvalues of $H^{\rm dis} - H_I^{\rm dis}$ are E_n, $E_n + \hbar c k_{ij}$, $E_n + \hbar c k_{ij} + \hbar c k_{lm}$, etc. When the λ_{nm}'s are small, one can expect the eigenvalues of $H^{\rm dis}$ to be close to the preceding ones. Then, except for particular values of the k_{ij}'s, only the eigenvalues of $H^{\rm dis}$ which are close to the E_n's are of the $\mathcal{R}$ type, in the sense of definition 1. Others are of the $\mathcal{C}$ type: when the coupling constant goes to 0, they tend to a linear combination of an atomic level's energy (possibly with the coefficient 0) with energies of a non-zero number of photons. In the particular two-level case, the excitation number operator $N := \sum_{n=0,1} |n\rangle\langle n| \otimes 1 + 1 \otimes a^*_{k_{01}} a_{k_{01}}$ commutes with $H^{\rm dis}$. Let $\mathcal{E}_l$ be the eigenspace associated with eigenvalue l of N. For $l \geq 1$, its dimension is 2. For example, for $l = 1$, $\mathcal{E}_1$ is spanned by $|0, k_{01}\rangle$ and $|1, \Omega\rangle$, Ω denoting the vacuum in the radiation space. In this case, the restriction of $H^{\rm dis}$ to $\mathcal{E}_1$ has two eigenvalues which are close to E_1 and $E_0 + \hbar c k_{01}$ respectively. We called the former $\mathcal{R}$-type and the latter $\mathcal{C}$-type resonances. If the photon energy k_{01} equals $E_1 - E_0$ (resonance), then the coupling $H_I^{\rm dis}$ removes the degeneracy of the eigenvalue of $H^{\rm dis} - H_I^{\rm dis}$ associated with eigenvectors in $\mathcal{E}_1$, and this is called the vacuum Rabi splitting. For this special value of the photon's energy, the $\mathcal{R}$-type and $\mathcal{C}$-type eigenvalues turn into the doublet of the VRS.

The number of eigenvalues of $H^{\rm dis}$ is infinite. Note that even the number of $\mathcal{R}$-type eigenvalues is greater than the number of discrete states, since the displacements of E_1 calculated in the $\mathcal{E}_l$'s are a priori different. This is also true for the resonances these eigenvalues change into in the non-zero width case. We know (see [19], for instance) that for two levels, with the coupling function $g(p) \sim p/(1 + p^2)$, there is a $\mathcal{R}$-type resonance and a $\mathcal{C}$-type one for the restriction of Hamiltonian (3) to each $\mathcal{E}_l$.

When the width of the g_{nm}'s is not zero, we expect the eigenvalues either to remain eigenvalues or to become resonances. If the detuning is large, that is to say if the photons' energy is not resonant with any atomic transition, and if the coupling constant is small, then resonances which were of the $\mathcal{C}$ type at zero width will remain so if the width is sufficiently small. For example, for $r \neq l$, eigenvalues close to $E_r + (l - r)k_{ij}$ will remain $\mathcal{C}$-type resonances.

In this setting, one may not see any reason for distinguishing two types of resonances if $\mathcal{C}$-type resonances were simply perturbed values of eigenvalues which have a simple physical meaning. The reason for such a distinction is twofold. First, the labelling is useful in cases where $\mathcal{C}$-type resonances of this kind are not obvious. It is the case for a large width continuum. An example is the case of an atom in the vacuum. The resonances of this $\mathcal{C}$-type are very different from the atomic energy levels and we need a term to label them. The term is kept in other cases. We will see that $\mathcal{C}$-type resonances disappear without trace when $\lambda = 0$. Second, some $\mathcal{C}$-type resonances are also of an other kind, as we will show it in Appendix A.

We are now going to study the two-level case more thoroughly. We are going to vary different parameters of the coupling of $\mathcal{S}$ to $\mathcal{C}$ and to follow the trajectories of some resonances under these variations.

2.4 Study of a two level system

We consider a two-level system in the rotating wave approximation (RWA). So there is only one coupling function g. Let $E_1 > 0$ be the energy of the excited state $|1\rangle$ and let us assume that the energy of the fundamental state $|0\rangle$ is 0. The Hamiltonian is

$$H = E_1|1\rangle\langle 1| \otimes 1 + 1 \otimes H_{\rm rad} + \lambda\Big(|0\rangle\langle 1| \otimes \big(a(g)\big)^* + |1\rangle\langle 0| \otimes a(g)\Big). \quad (6)$$

We assume that $||g||_2 = 1$, the strength of the coupling appearing in λ, which has the dimension of an energy.

As the resonances can only be obtained by computer, we are going to chose a particular g. This example will yield the important notions. The chosen function is

$$g(k) := \sqrt{\frac{2}{\pi}} \frac{(\mu k_0)^{-1/2}}{1 + \mu^{-2}(\frac{k}{k_0} - 1)^2}. \quad (7)$$

As μ gets smaller, the function becomes more peaked at $k_0 > 0$ (the width is $2\mu k_0$, see Fig. 2). We set $\delta := E_1/(\hbar c k_0) - 1$; $\delta \in]-1, \infty[$. Physically, this function for example models the effect of a cavity, in the $\mathcal{S}$-field interaction, μ being proportional to the inverse of the cavity's quality factor and k_0 being a particular cavity's mode. When g is very peaked at k_0, δ measures the detuning between the levels' spacing and the energy of the coupled photons. We will only consider eigenvalues or resonances of the restriction of H to $\mathcal{E}_1$ (defined in Sect. 2.3). They are zeros of

$$z \to z - E_1 - \lambda^2 \int_{-\infty}^{+\infty} \frac{g(k)^2}{z - \hbar c|k|} dk \quad (8)$$

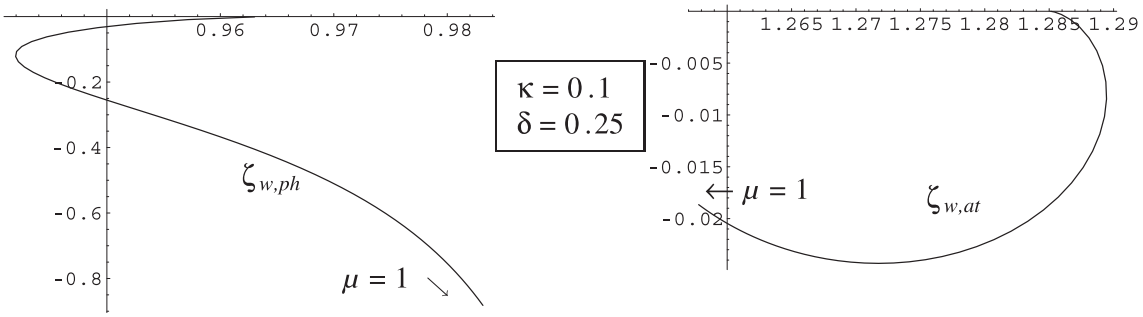

Fig. 1. Values $\zeta = (\hbar c k_0)^{-1} z$, for two resonances z, μ varying from 0.01 to 1.

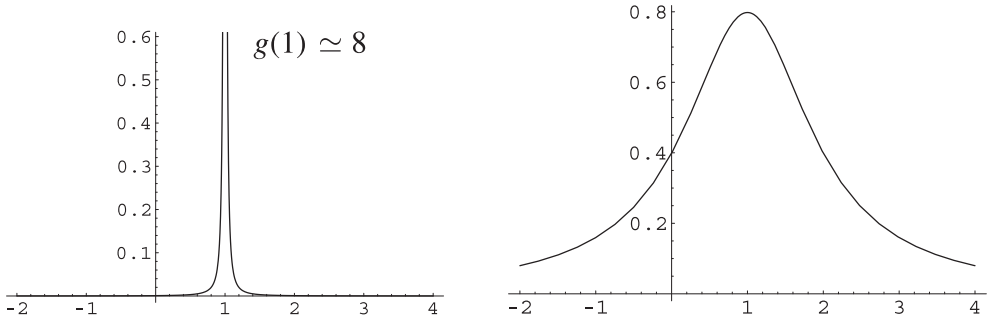

Fig. 2. The coupling function for $\mu = 0.01$ (left) and for $\mu = 1$ (right). Units are k_0 on the abscissa and $k_0^{-1/2}$ on the ordinate.

or of its analytic continuation into the lower complex half-plane, across the cut $\mathbb{R}^+$. (For $z = E_1$, the integral term in (8) is simply the correction to the upper level's energy due to the emission and re-absorption of a virtual photon.) With $\kappa = (\hbar c k_0)^{-1}\lambda$ and for $\zeta < 0$, let us set

$$f(\kappa,\mu,\delta,\zeta) := \zeta - (1+\delta) - \frac{2\kappa^2}{\pi\mu}\int_{-\infty}^{+\infty} \frac{1}{\left(1+(\frac{y-1}{\mu})^2\right)^2}\frac{1}{\zeta-|y|}dy. \quad (8')$$

The resonances we are interested in are the product of $\hbar c k_0$ and zeros of the analytic continuation $f_+(\kappa,\mu,\delta,.)$ of $f(\kappa,\mu,\delta,.)$ into the lower complex half-plane.

We are now going to study the position of these zeros as functions of three physical parameters of the system: κ, μ and δ. An important point has to be mentioned: when at least two variables are considered, the position of these zeros is a multivalued function of these variables, even if these variables remain real [21]. This leads to a complication as regards the zeros' notation.

2.4.1 Displacement of two resonances through the variation of the coupling function's width

We start with a study with clearly non-zero detuning in order to study the effect of the variation of the continuum's width independently of resonance effects (here this word means zero detuning).

When μ tends to 0, it can be shown that $f(\kappa,\mu,\delta,\zeta)$ and $f_+(\kappa,\mu,\delta,\zeta)$ tends to $\zeta - 1 - \delta - \kappa^2/(\zeta-1)$. For small κ, one of the zeros of this function is close to $1+\delta$ (resonance close to E_1) and the other one is close to 1 (resonance close to $E_0 + \hbar c k_0$). The zeros of $f_+(\kappa,\mu,\delta,\zeta)$ generated by the preceding zeros when μ increases, starting from 0, are denoted respectively by $\zeta_{w,at}(\mu)$ and by $\zeta_{w,ph}(\mu)$. The index w indicates that only the width varies; δ and κ remain constant. Subscripts "at" and "ph" indicate that if $\mu \to 0$ and then $\kappa \to 0$, the limits are the energy of the atom's excited state and the energy of the photon, respectively. Let us mention that $f_+(\kappa,\mu,\delta,.)$ has another zero for $\mu \neq 0$, whose physical meaning is no more obvious. It is described in Appendix A.

For $\kappa = 0.1$ and $\delta = 0.25$, the position of two resonances when μ is varied is given by the curves of Figure 1.

Limits of $\zeta_{w,ph}(\mu)$ and $\zeta_{w,at}(\mu)$ for μ tending to 0 are respectively $1 + 2^{-1}(\delta - (\delta^2+4\kappa^2)^{1/2}) = 0.965$ and $1 + 2^{-1}(\delta + (\delta^2+4\kappa^2)^{1/2}) = 1.285$.

The coupling functions for $\mu = 0.01$ and $\mu = 1$ are plotted in Figure 2.

In Figure 1 we see that the imaginary part of $\zeta_{w,at}$ does not exceed 0.03 in modulus whereas that of $\zeta_{w,ph}$ increases and takes much larger values when μ increases.

For small μ, the resonances are close to the real axis. However, let us note that $\zeta_{w,at}$ is here also much closer to the reals than $\zeta_{w,ph}$. Indeed, the calculation gives $\zeta_{w,at} = 1.285 – 2.7 \times 10^{-6} i$ and $\zeta_{w,ph} = 0.963 – 9.8 \times 10^{-4} i$ for $\mu = 0.01$.

Before we turn to the $\mu \to 0$ limit, let us comment on the type of $\zeta_{w,at}(\mu)$ and $\zeta_{w,ph}(\mu)$, with the same values of κ and δ. Since, by a continuity argument, $\zeta_{w,ph}$ and $\zeta_{w,at}$ remain respectively in neighbourhoods of 0.965 and 1.285 when μ is small, $\zeta_{w,at}(\mu)$ is of the $\mathcal{R}$-type for small μ, whereas $\zeta_{w,ph}(\mu)$ is of the $\mathcal{C}$-type. Indeed, the energy of $|1\rangle$ is 1.25, in $\hbar c k_0$ units, and it is actually the zero of f

sitting at $\zeta_{w,at}(\mu)$ for $\kappa = 0.1$ which tends to 1.25 when κ tends to 0. In Section 2.4.3.2, we show what happens when μ increases. Physically, when μ gets sufficiently large, the detuning is no longer noticeable and, if the coupling is strong enough, we may expect that the atomic and photonic states be mixed, and even hardly distinguishable. As a consequence, if μ is large, it is difficult to guess which of the two resonances goes to 1 and which goes to $1+\delta$, when κ goes to 0. In other words it is difficult to guess which is the $\mathcal{R}$-type one. In Section 2.4.3.2, we even show that for some value of κ and μ, both resonances coincide.

In the $\mu \to 0$ limit, the Hamiltonian formally becomes

$$H_1 = E_1|1\rangle\langle 1| \otimes 1 + 1 \otimes H_{\rm rad} + \lambda(|0\rangle\langle 1| \otimes a_1^* + |1\rangle\langle 0| \otimes a_1) \tag{9}$$

where a_1 is the annihilator of a photon with energy $\hbar c k_0$. Photons whose wave numbers differ from k_0 are decoupled. Let us consider the reduced Hilbert space $\mathcal{H}_0$, tensor product of $\mathcal{H}_S$ and the k_0-photon's Fock space. The restriction of H_1 to $\mathcal{H}_0$ has an infinite number of eigenvalues. They are of the form $z_{\pm,n} = \hbar c k_0 \zeta_{\pm,n}$, with

$$\begin{aligned} \zeta_{-,n} &= n + 2^{-1}(\delta - \sqrt{\delta^2 + 4n\kappa^2}), \\ \zeta_{+,n} &= n + 2^{-1}(\delta + \sqrt{\delta^2 + 4n\kappa^2}). \end{aligned} \tag{10a}$$

The associated eigenvectors are

$$\begin{aligned} \phi_{\pm,n} = \big(1 + n\kappa^2 \zeta_{\pm,n}^{-2}(\kappa)\big)^{-1} \Big(&|1\rangle \otimes |k_0\rangle^{\otimes n} \\ &+ \sqrt{n}\kappa \zeta_{\pm,n}^{-1}(\kappa) |0\rangle \otimes |k_0\rangle^{\otimes (n-1)} \Big). \end{aligned} \tag{10b}$$

The coupling thus yields dressed states. When κ goes to 0, $\phi_{+,n}$ tends to $|0\rangle \otimes |k_0\rangle^{\otimes n}$ for $\delta > 0$ and to $1 \otimes |k_0\rangle^{\otimes (n-1)}$ for $\delta < 0$. It is the other way round for $\phi_{-,n}$.

These dressed states do not exist anymore as eigenstates of the Hamiltonian when the coupling function has a certain width. The eigenvalues, i.e. the energies of these states, turn into the resonances drawn in Figure 1. They both acquire an imaginary part.

In the non-zero width case, let us now look at what happens when the two levels' spacing is varied around $\hbar c k_0$.

2.4.2 Variation with respect to the detuning. The levels' anti-crossing

(a) The discrete case

Let us first recall what happens in the case where the width of g is zero. When δ varies, both energies (10a) of the dressed states corresponding to $n = 1$ vary. When δ tends to $\pm\infty$, they asymptotically tend to the energies of states $|0\rangle \otimes |k_0\rangle$ and $1 \otimes |0\rangle$. These limits (in $\hbar c k_0$ units) are drawn in dashed lines in Figure 3, for $\kappa = 0.1$. They cross when $E_1 = \hbar c k_0$.

We see that the interaction yields what is called an anti-crossing, for whatever value of the coupling constant. The larger the coupling constant, the larger the repulsion

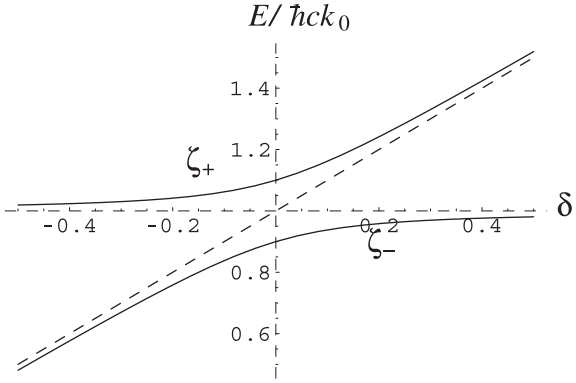

Fig. 3. The levels' anti-crossing, for an infinitely narrow continuum.

of the two curves, since the energies at $\delta = 0$ are separated by 2κ. The same phenomenon repeats in the neighbourhood of n-photon resonances. We are now going to show how this anti-crossing is modified when the width of g is no longer zero. Let us note that (10a) shows that ζ_+ is of the $\mathcal{R}$-type whereas ζ_- is of the $\mathcal{C}$-type.

(b) The narrow continuum case

To each point on one of the two curves of the discrete case, there now corresponds, in the continuous case, a complex number. For example, for $\mu = 0.01$ and $\delta = 0.25$, the curves in Figure 1 give values $0.963–9.8 \times 10^{-4}$ and $1.285–2.7 \times 10^{-6}$. When δ varies, with the same μ value, the resonances move in the lower complex half-plane as is indicated in Figure 4.

In this figure, we see that the imaginary parts of both resonances are more or less the same for $\delta = 0$, about -9.5×10^{-5}. The one whose real part is greater than 1 will be denoted by ζ_+, the other by ζ_-. For both curves, it can be shown that the imaginary part tends to $-\mu = -0.01$ when the real part goes to 1 (we recall that $1 - i\mu$ is a pole of the integrand in $(8')$, coming from a pole of g).

We also see that ζ_+ is asymptotic to the reals when $\delta \to +\infty$. (It can be seen that it behaves like $1 + \delta$.) Conversely, ζ_- comes closer to the reals when δ decreases to -1, and tends to $1 - i\mu$ when $\delta \to +\infty$. One usually considers the imaginary part of the resonance associated with an excited atomic state as the energy half-width of this state, a state that the coupling has made unstable. In the same way here, we may say, as in the discrete case, that the resonance ζ_- tends to the photon's energy in the limit $\delta \to +\infty$, it being understood that this energy is spread over a width equal to 2μ. Note that such an interpretation would no longer hold for a wide continuum.

This leads us to propose to represent the mixed states' energies in the following way, which generalizes the diagram in Figure 5.

For each value of δ, a resonance is represented by a vertical line segment centered at the real part of the resonance and whose length is twice the imaginary part, i.e. the set $\delta + i[\Re\zeta - \Im\zeta, \Re\zeta + \Im\zeta]$.

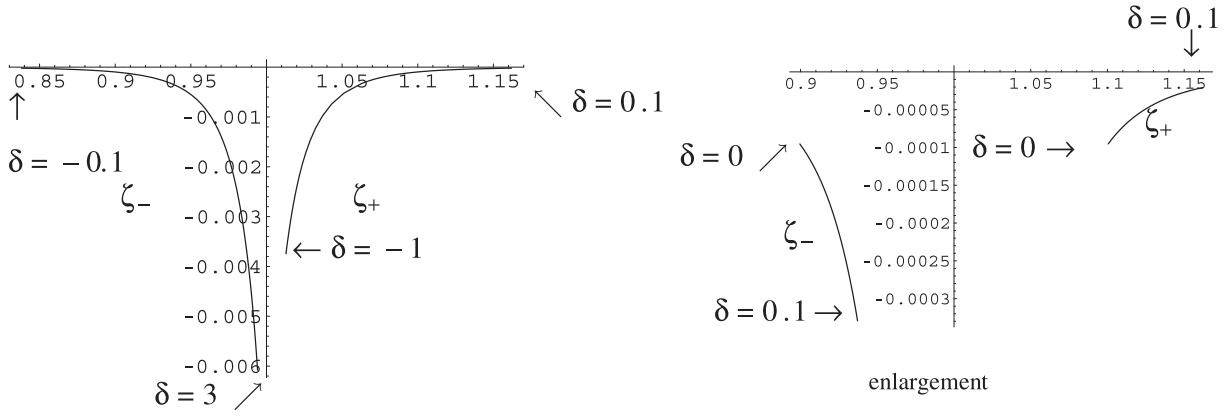

Fig. 4. Variation of two resonances in the complex plane, with respect to the detuning δ, for $\kappa = 0.1$ and $\mu = 0.01$ (expressed in $\hbar c k_0$ units).

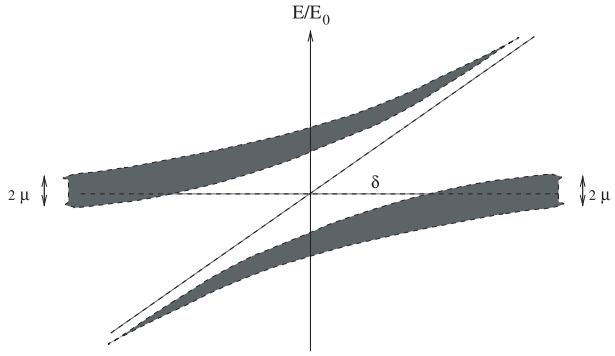

Fig. 5. Representation of two resonances in the real plane, as a function of the detuning, for $\kappa = 0.1$ and $\mu = 0.01$.

We are not going to determine the type of the two resonances. It may change when δ varies if μ is not close to 0.

(c) Discretization of the continuous case

In some papers, things are presented in an other way. The continuum is discretized into a set of photon wavevectors $k_1, ..., k_n$, with corresponding coupling constants $\lambda_1, ..., \lambda_n$. In the one-excitation space $\mathcal{E}_1$, we thus get an Hamiltonian whose only non-vanishing matrix elements are those between states $|1;0\rangle$ and $|0;k_i\rangle$. As an example, let us take three values for k, say $k_- := k_0(1-\mu), k_0, k_+ := k_0(1+\mu)$ and coupling constants $\lambda_- := \frac{1}{2}\kappa\hbar c k_0, \lambda_0 := \kappa\hbar c k_0, \lambda_+ := \frac{1}{2}\kappa\hbar c k_0$. Then, in the $\{|1;0\rangle, |0;k_-\rangle, |0;k_0\rangle, |0;k_+\rangle\}$ basis, the Hamiltonian's matrix is

$$M = \hbar c k_0 \begin{pmatrix} 1+\delta & \kappa/2 & \kappa & \kappa/2 \\ \kappa/2 & 1-\mu & 0 & 0 \\ \kappa & 0 & 1 & 0 \\ \kappa/2 & 0 & 0 & 1+\mu \end{pmatrix}.$$

Let us set $\kappa = 0.1$ and $\mu = 0.01$, as before. The variation with δ of the four eigenvalues of M is given in Figure 6.

It can be shown that the four curves do not cross. Therefore, it is $\hbar c k_+$, the greatest of the three eigenvalues in the continuum for $\delta \to -\infty$, which tends to the energy of state $|1\rangle$ when $\delta \to +\infty$. Conversely, it is $\hbar c k_-$, the smallest of the three eigenvalues in the continuum for $\delta \to +\infty$, which tends to the energy of state $|1\rangle$ when $\delta \to -\infty$. The description we gave in the continuous case is a concise rigorous way of conveying what may be approached by such discretizations.

Looking back at Figure 5, a visualization of Figure 4, we see that we get states which are not only mixed states, but also, in a sense, enlarged states. Let us now look at the dependence with respect to λ. It will enable us to examine the notions of strong and weak coupling regimes in the light of the preceding results.

2.4.3 Variation with the coupling constant

2.4.3.1 A change in the regime around a critical value

Let us qualitatively see what is expected. When κ decreases, μ being fixed, the two grey tinted regions of Figure 5 approach each other. Since their widths at each end do not depend on κ, the line segments at $\delta = 0$ are going to overlap. The situation is then that of Figure 7a. The calculation shows (see below) that for a certain κ_c, the two line segments at $\delta = 0$ coincide (same energy at the center and same length, i.e. the resonances coincide in the complex plane). When κ decreases and crosses this value, Figure 7a changes in a continuous way into Figure 7b.

The two regimes called "strong coupling regime" and "weak coupling regime" in the literature clearly appear in this picture, on each side of κ_c. In the weak coupling regime, the labelling $\zeta_\pm$ is no longer pertinent. However, one of the two resonances can be associated with the atom and the other one with the photon. This is translated in the notations ζ_{phot} and ζ_{atom}. When the coupling increases beyond the critical value, this labelling is no longer possible. The mixing of the states is important when the detuning is close to zero. An atomic state is changed continuously into a photonic state when the detuning increases from -1 to 1. Moreover, Figure 7a shows that ζ_+ becomes more and more unstable as δ decreases to 0, in the same

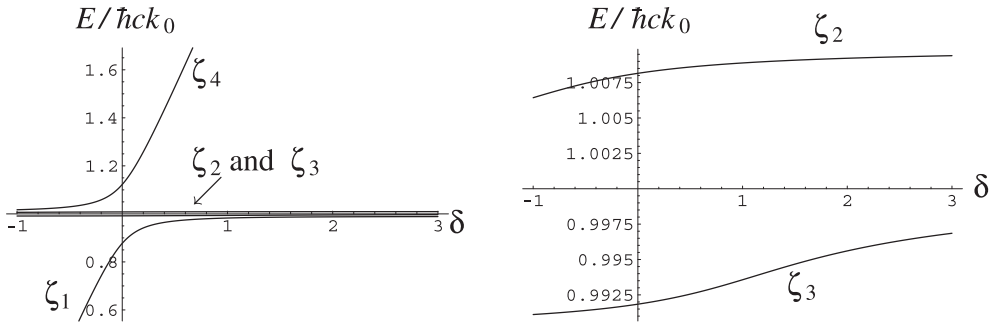

Fig. 6. Four eigenvalues of the Hamiltonian, when the continuum is replaced by three discrete values (in $\hbar ck_0$ units). $\kappa = 0.1$.

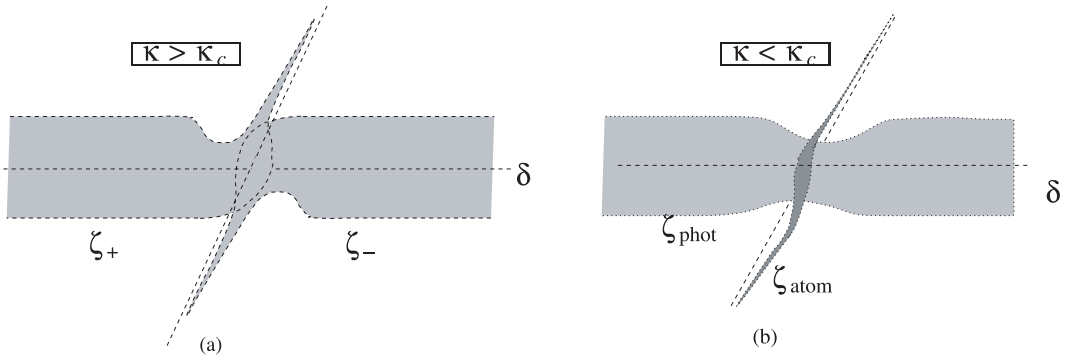

Fig. 7. Variation of the resonances' energies with respect to the detuning, at the transition between the strong (a) and weak (b) coupling regimes. A real representation.

way as ζ_{atom} did for $\kappa < \kappa_c$, in Figure 7b. These emission enhancements are well-known physical facts.

The preceding description gives a picture of the displacement of the two resonances in the complex plane. For $\mu = 0.01$, the critical value of κ is close to 3×10^{-3}.

In Figure 8, we show the exact position of each resonance, as a function of the detuning, in the two regimes. The dotted parts of the curves are obtained through varying δ step by step; the points have not been joined by a curve so as to underline the rapid variation near the singular point.

For a given μ, the critical value $\kappa_c(\mu)$ can be obtained analytically through looking for κ and δ values for which $f_+(\kappa, \mu, \delta, .)$ has a double zero. It amounts to solving the four equations

$$\Re f_+(\kappa,\mu,\delta,\zeta) = 0 \qquad \Im f_+(\kappa,\mu,\delta,\zeta) = 0$$

$$\Re \partial_\zeta f_+(\kappa,\mu,\delta,\zeta) = 0 \qquad \Im \partial_\zeta f_+(\kappa,\mu,\delta,\zeta) = 0$$

for the four unknown $\kappa, \delta, \Re\zeta$ and $\Im\zeta$, with

$$f_+(\kappa,\mu,\delta,\zeta) = \zeta - 1 - \delta - \kappa^2 \left[\frac{2}{\pi} \int_{-\infty}^{-\frac{1}{\mu}} \frac{dy}{(1+y^2)^2(\zeta+1+\mu y)} + \frac{2}{\pi} \int_{-\frac{1}{\mu}}^{\infty} \frac{dy}{(1+y^2)^2(\zeta-1-\mu y)} + \frac{4i}{\mu} \left(\frac{1}{(1+\mu^{-2}(\zeta+1)^2)^2} + \frac{1}{(1+\mu^{-2}(\zeta-1)^2)^2} \right) \right].$$

On a computer, one indeed finds $\kappa_c = 0.003, \zeta = 1 - 0.0038i$ and $\delta \simeq 0$.

From Figure 8, it is clear that, for $\delta = 0$, ζ_{atom} is of the $\mathcal{R}$ type whereas ζ_{phot} is not. Indeed, the curve ζ_{atom} is going to flatten on the reals as κ decreases, ζ_{atom} moving to 1, whereas it can be shown that ζ_{phot} moves towards $1 - i\mu$, being therefore of the $\mathcal{C}$-type. In the weak coupling regime, the curves representing the resonances' real parts cross as the detuning varies, whereas we have an anti-crossing in the strong coupling regime. The distinction between the two regimes requires a detailed analysis near $\delta = 0$. Such an analysis at resonance can be found in [22] for the case of excitons in semiconductor microcavities.

One could also look at the regime's transition through varying μ, κ being fixed. The strong coupling regime would then occur below a critical μ, depending on κ. Note that the ratio κ_c/μ is about 0.3 for the μ value we considered.

We take this example as a model in defining the two regimes for the coupling of a two level system $\mathcal{S}$ to a continuum.

Definition 2*: we say that we are in a strong coupling regime if, through the variation of the detuning between $\mathcal{S}$ and the continuum, the two resonances move as it is represented in Figure 7a or Figure 5. We are in a weak coupling regime if the two resonances move as it is represented in Figure 7b.*

Note that this definition depends on the existence of a parameter measuring the detuning and that it therefore does not apply when this parameter is no longer obvious.

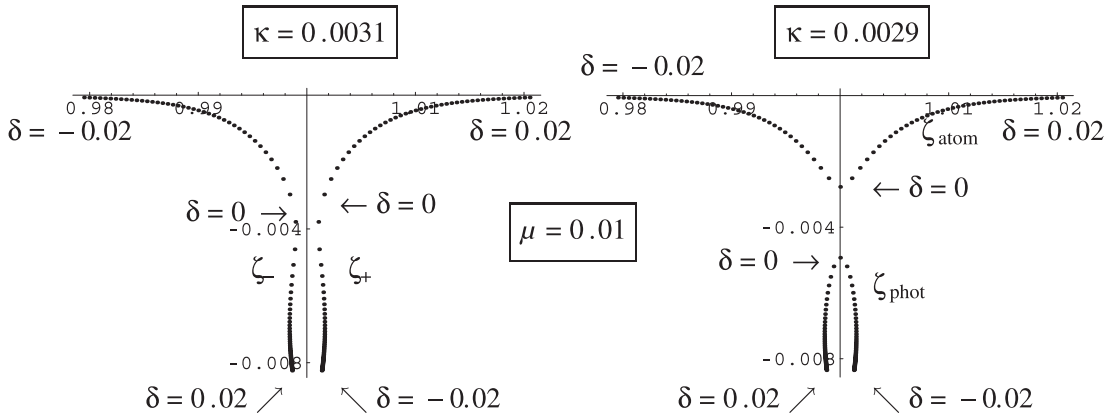

Fig. 8. Variation of the resonances' energies with respect to the detuning, at the transition between the strong and weak coupling regimes. Representation in the complex plane of $\zeta = E/(\hbar c k_0)$.

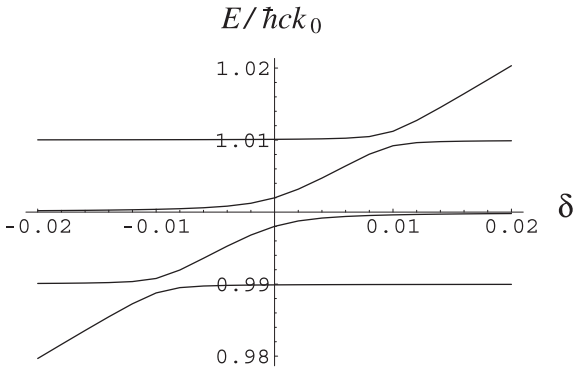

Fig. 9. Variation of four eigenvalues, at $\kappa = 0.002$, for a discretization of the continuum. $\mu = 0.01$.

In Section 4, we introduce the coupling function $-\sqrt{3}(1+(k/k_0)^2)^{-2}k/k_0$, the atom level-spacing being 1; in this case there is no obvious detuning parameter.

When the continuum is coarsely discretized into three levels as before, there is no critical κ, but the atomic states gradually shows up when the coupling constant decreases. For instance, Figure 9 describes what Figure 6 becomes when $\kappa = 0.002$.

2.4.3.2 The $\lambda \to 0$ behaviour of resonances sitting at $\zeta_{w,ph}(\mu)$ and $\zeta_{w,at}(\mu)$

It can be checked by computer, up to $\mu = 5$, that $\zeta_{w,ph}(\mu)$ is of the $\mathcal{C}$ type and that $\zeta_{w,at}(\mu)$ is of the $\mathcal{R}$ type.

2.4.3.3 Behaviour of resonances sitting at $\zeta_{w,ph}(\mu)$ and $\zeta_{w,at}(\mu)$ when the coupling increases

Let us consider the resonance which sits at $\zeta_{w,ph}(0.01)$ when $\kappa = 0.1$ and follow its trajectory as κ increases. We find that its real part decreases and that its imaginary part also decreases, down to a value around $0.11–2\times10^{-6}i$ for $\kappa \simeq 1.0062$. Let us call $\mathcal{R}$ the curve segment thus drawn. This reminds us of the behaviour that we mentioned in the introduction, a behaviour that we illustrated elsewhere [21], with the function $g(p) = \sqrt{2/\pi}\,p/(1+p^2)$: in that case, the analogous resonance became real negative beyond a certain value of κ. The existence of this eigenvalue has been known for a long time ([23], C_{III}.6 of [24]). In the present case the resonance does not become real; its imaginary part starts growing beyond the above-mentioned value of κ. Nevertheless, for large κ, greater than 1.2 for instance, one can see that there does exist a negative eigenvalue of the Hamiltonian. It approaches 0 when κ decreases to 1.118 and connects to $\mathcal{R}$, but only if κ follows a path avoiding a neighbourhood of 1.1, in the complex plane. This indicates a branch point of the zeros of the multivalued function f, in this region of the κ complex plane. A complication may be due to the following fact. There is a difficulty for a zero of f to cross 0: for $\zeta \sim 0^-$, the integral in (8′) diverges, because g does not vanish at 0, contrary to the above-mentioned case. It would be interesting to multiply the coupling function (7) by p and see whether the negative eigenvalue reaches 0, which is likely to be the case.

The resonance which sits at $\zeta_{w,at}(0.01)$ for $\kappa = 0.1$ tends to the positive real axis at infinity, after having moved away from it for a while.

We are now going to go through several subjects concerning mixed states (also called intricate, or hybrid states in the literature) and the two coupling regimes, for interactions of a discrete-level system with a continuum. These subjects have been often studied in the last years and there still is an intense experimental activity in these domains. In each of these examples, the three parameters we used before will come into play.

3 Illustration of the general study in several concrete cases

3.1 Atoms (or equivalents) in cavities. The continuum is a continuum of photon states

Let us consider an atom with two levels (states $|0\rangle$ and $|1\rangle$), in resonance with the mode of a cavity with quality factor Q. Let ω be the angular frequency of the photons.

We refer to the introduction for some works on cavity electrodynamics. One may also consult Haroche's courses at College de France (2001–2004), which are accessible, for recent studies. The strength of the atom-mode coupling is measured by the frequency $\frac{1}{\hbar}D_{10}\sqrt{\hbar\omega/(2\epsilon_0 V)}$, D_{10} being the matrix element of the electric dipole operator between the two states and V the cavity's volume. Since the cavity is not perfect, the mode may be described as an environment presenting a Lorentzian spectrum with width $\Gamma_c = \omega/Q$ to the atom. When Q is large, we are in the small μ case of the general presentation and thus in a strong coupling regime. In the $\Gamma_c = 0$ limit, and with at most one photon present, we are in the case of Figure 3: the coupling yields intricate atom-photon eigenstates (polariton states), which are linear combinations of $|0, 1 \text{ photon}\rangle$ and $|1, 0 \text{ photon}\rangle$ states. If Γ_c is not considered as zero, these states become the two resonances described in the general presentation. We are in the case of Figure 5. The width at infinity on the abscissa axis is 2Γ. The complex values of the resonances, and in particular their imaginary parts, vary with the detuning. When the detuning changes from a large negative value to a large positive one, a "photonic state" changes continuously into an "electronic state" or conversely, depending on which resonance is considered. We get there intricate states which have been much studied these last years. Rydberg atoms are specially appropriate to the study of this atom-cavity strong coupling [13]. Studies are presently conducted on this subject. It might be useful to look at the resonances' position in the complex plane to get a more precise description than the approximation given by Figure 3.

In Section 4 we examine what becomes of the resonances in a case where the cavity is no longer present.

We find an analogous situation for excitons in semiconducting microcavities [10,11,25]. One can vary the photon continuum's width (through changing the cavity's quality factor) or the coupling strength (for example by means of a magnetic field ([10] p. 43), so as to pass from the strong to the weak coupling regime. In the former, the experimental curves show two peaks, whereas in the latter, they often show only one peak. Since we did find two resonances in both regimes, we must explain this. Three reasons may be put forward. The first one is that one resonance's imaginary part may become large (widening of the peak which disappears). The second is that one resonance may stay out of the energy range which the apparatus tests. A third possibility is that the probe be sensitive to the cavity's state and not to the exciton's state (see [14] Sect. 3.3, for the atom-and-cavity case).

The excitons may also acquire a certain width, through exciton-exciton or exciton-phonon interactions, but we do not consider interactions of two continuums in this paper.

3.2 Excitons in a microcavity. A case where the continuum consists of excitonic states

Let us now assume that the photon in the cavity is practically monochromatic. We may have the exciton's energy spectrum seen by the photon varying by means of a magnetic field. The spectrum has a discrete part and a continuous part and both changes with the magnetic field. When the photon energy is in the discrete part of the exciton's spectrum, we get several possible resonances, with small width, and the anti-crossings when two different exciton-photon states have neighbouring energies. When the photon energy is in the continuous part of the exciton spectrum, the photon energy gets widened [12].

The first situation corresponds to the strong coupling regime of Figure 3, for each anti-crossing. Both resonances at stake at each anti-crossing have a small width. None of them can be associated with the photon or with the exciton if the detuning is not large. Corresponding mixed states are called magnetopolaritons. In the second situation, experimental curves show that the coupling to the continuum gives the photon state a certain width ([12] Fig. 2). Through calculating the displacement in the complex plane of the photonic resonance, as the detuning passes from a negative value (not too big, the photon's energy has to stay in the continuum) to a positive one, one should get the same picture as for ζ_{atom} in Figure 7b.

3.3 Electron-phonon mixed states

An other example where ideas developed in Section 2 apply, although with some modifications, is the coupling of electrons confined in quantum dots to longitudinal optical phonons of a bi-atomic lattice. The interaction is that of the electron with the electric field created by the lattice dipoles, a field which oscillates according to the various possible modes. The Frölich Hamiltonian of the electron-phonon system formally reads

$$H_{\text{el}-\text{ph}} = \sum_{n\geq 0} E_n |n\rangle\langle n| \otimes 1 + 1 \otimes \sum_{\mathbf{k}\in\mathcal{B}} \hbar\omega(k) a^*_{\mathbf{k}} a_{\mathbf{k}} + \mathcal{N}^{-1/2} C \sum_{\mathbf{k}\in\mathcal{B}} k^{-1} (a^*_{\mathbf{k}} e^{-i\mathbf{k}\cdot\mathbf{r}} - a_{\mathbf{k}} e^{i\mathbf{k}\cdot\mathbf{r}}) \quad (11)$$

where $|n\rangle$, $n = 0, 1, \cdots$ denotes the eigenstates of the electron in the dot, $\omega(\mathbf{k})$ is the energy of a phonon with wave number $\mathbf{k}$, $\mathcal{B}$ is the first Brillouin zone, C is a pure imaginary constant and $\mathcal{N}$ a normalization factor ([26] p. 656). If the lattice is infinite, the possible values of $\mathbf{k}$ make a continuum and the Hamiltonian may be written

$$H_{\text{el}-\text{ph}} = \sum_{n\geq 0} E_n |n\rangle\langle n| \otimes 1 + 1 \otimes H_{\text{phon}} + \sum_{m,n} \lambda_{mn} \big(|m\rangle\langle n| \otimes a^*(\overline{g}_{mn}) + |n\rangle\langle m| \otimes a(g_{mn}) \big) \quad (12)$$

where H_{phon} is the energy operator in the phonon space: $H_{\text{phon}} = \hbar \int_{\mathcal{B}} \omega(k) a^*_{\mathbf{k}} a_{\mathbf{k}} d\mathbf{k}$ and

$$g_{mn}(\mathbf{k}) := i \Big(\int_{\mathcal{B}} |k|^{-2} |\langle m| e^{i\mathbf{k}\cdot\mathbf{r}} |n\rangle|^2 d\mathbf{k} \Big)^{-1/2} \times |k|^{-1} \langle m| e^{i\mathbf{k}\cdot\mathbf{r}} |n\rangle \quad (13)$$

are the (normalized) coupling functions; the coupling constants

$$\lambda_{mn} = (2\pi)^{-3/2} iC\Big(\int_{\mathcal{B}} |k|^{-2} |\langle m|e^{i\mathbf{k}\cdot\mathbf{r}}|n\rangle|^2 d\mathbf{k}\Big)^{1/2} \quad (14)$$

have the dimension of an energy. In calculating eigenvalues of $H_{\mathrm{el-ph}}$, one often limits oneself to considering two particular levels $|0\rangle$ and $|1\rangle$, for example the first two levels of the dot, also neglecting the Hamiltonian's matrix elements which are of order greater than one. In [6], one of the strong coupling regime exhibited involves states (s, 1 LO phonon) and (p, 0 LO phonon) for electrons in InAs quantum dots. Let us consider this approximation and this example. Function $\omega(\mathbf{k})$ is maximum for $\mathbf{k} = 0$, where it is equal to 36 meV. The range of $\omega(\mathbf{k})$ is 8 meV. Actually, if we take account of the k^{-1} dependence of the interaction and limit ourselves to $\mathbf{k}$'s which give appreciable values of the matrix elements, the range reduces to 0.4 meV. The electron-phonon detuning is obtained through varying the quantum levels in the dot by means of a magnetic field. Let us denote the level spacing by $E(\delta) := \hbar\omega_0(1+\delta)$, δ measuring the detuning with respect to the photon energy mean value $\hbar\omega_0$. The Hamiltonian is

$$H = E(\delta)|1\rangle\langle 1| \otimes 1 + 1 \otimes H_{\mathrm{phon}} + \lambda\big(|1\rangle\langle 0| \otimes a^*(\overline{g}) + |0\rangle\langle 1| \otimes a(g)\big) \quad (15)$$

where $g = g_{01}$ and $\lambda = \lambda_{01}$. If $\omega(\mathbf{k})$ had only one value ω_0, the eigenvalues would be roots of equation $z - E(\delta) - \lambda^2/(z - \hbar\omega_0) = 0$. Indeed, eigenvalues or resonances are obtained by means of the function

$$f(\lambda, \delta, z) := z - E(\delta) - \lambda^2 \int_{\mathcal{B}} \frac{|g(\mathbf{k})|^2}{z - \hbar\omega(\mathbf{k})} d\mathbf{k}. \quad (16)$$

They are its zeros or those of some analytic continuation in the lower half-plane. When the phonon continuum is infinitely narrow, the zeros are therefore real and there variation with δ is of the type shown in Figure 3. When the width is no longer 0, it is interesting to see whether resonances are described by Figure 5 or Figure 7b, i.e. whether the coupling regime is strong or weak. Interpreted in the subspace spanned by states (s, 1 LO phonon) and (p, 0 LO phonon), data given in [6] for the energies of stationary states, or almost stationary states (see the remark just below and in the next to last paragraph of this section), show that we are not in the case of Figure 7b, but in a strong coupling regime. As a consequence, when δ passes from a large negative value to a large positive one, a phonon state changes continuously into an electronic state. Let us note that the smallness of the continuum's effective width, and also the limit in the measurements' precision imply that points which should be represented in a figure of Figure 5-type are actually represented as in Figure 3.

There is a difference between this problem and that of the coupling of a discrete system to the photon. In the present case there are two functions which contribute to the resonances' imaginary part: g and ω. In the limit $\delta \to \infty$, the vertical extension of the lower surface of Figure 5, which expresses the imaginary part of one of the resonances, depends on both widths. Only explicit calculations would tell us how the widths of these two functions (and even the functions themselves) contribute to the final result.

Unfortunately, a numerical calculation is more complicated than in the case where $\omega(\mathbf{k}) = |k|$. It has not been done. Indeed, performing an analytic continuation requires knowing the values $\mathbf{k}_1(z), \mathbf{k}_2(z), ...$ for which $\omega(\mathbf{k}) = z$. Even in the case where $\omega(\mathbf{k})$ has an explicit form, the $\mathbf{k}_i(z)$ are not simple functions. For example, for a one-dimension lattice with equal mass atoms, the $\mathbf{k}_i(z)$ are of the form $\arccos(cz)$, a function which is multivalued. Nevertheless, let us show qualitatively how $\omega(.)$ may create a resonance distinct from the one which is close to $E(\delta)$ when the coupling constant is small. In one dimension, and in the case of equal mass atoms, we have $\omega(k) = \omega_{\max}\cos(ak/4)$, with a the lattice spacing. Therefore, values taken by ω lie in $I =]\frac{\sqrt{2}}{2}\omega_{\max}, \omega_{\max}]$. When z, coming from the upper half-plane, crosses this interval at a point different from $\hbar\omega_{\max}$, the integrand's denominator in (16) has two poles in the integration interval, $]-\pi/a, \pi/a]$, which are $\pm\arccos((\hbar\omega_{\max})^{-1}z)$; the integration interval can be deformed so as to avoid these two poles whereas this is not the case if z comes to $\hbar\omega_{\max}$, the integral becoming divergent. $z = \hbar\omega_{\max}$ is thus a singularity. Let us assume it be the only one and, moreover, a simple pole. By analogy with the expression $z - E(\delta) - C^{\mathrm{te}}\,\lambda^2/(z - \hbar\omega_{\max})$, we may expect a zero of $f(\lambda, \delta, .)$ near $\hbar\omega_{\max}$, for λ small. The zero of $f(\lambda, \delta, .)$ will in fact be complex because the continuation of that function is complex. Let us recall other singularities of the continuations of $f(\lambda, \delta, .)$, already met in the photonic case. They are due to poles of g. For example, if k_p is a pole of g in the lower half-plane, $\omega(k_p)$ may be a singular value of some analytic continuation of $f(\lambda, \delta, .)$.

Nevertheless, from general ideas deduced from the analysis of Section 2, one can make two points. Firstly it is because the continuum is narrow that the strong coupling regime occurs, the coupling then resembling that of discrete states, with real energies. Secondly, there is an important difference with this latter case: the width of the phonon states' continuum, as small as it may be, makes the dressed electron-phonon states unstable, since the energies of these states now have a nonzero imaginary part. In the same way, the photons, although they are stable, give an imaginary part to the electron energies of the naked atom, through the extension of their spectrum. This remark may be useful in discussing the stability of polarons.

An analogous situation occurs in the case of the exciton-phonon coupling in semi-conductor quantum dots (excitonic polarons) [4,5].

In most of the preceding cases, data are obtained only for narrow continuums. As a consequence, $\mathcal{C}$-type resonances, for example ζ_{phot} at $\delta = 0$ in Figure 8, do not appear as something special or are expected to be negligible (see the comment at the end of Appendix A). We now

want to show these resonances in less trivial situations, in which the $\mathcal{C}$-type resonances are not a priori close to the reals. To do so, we will be concerned with a wide continuum. We shall take the example of the hydrogen atom coupled to the electromagnetic field in the vacuum.

4 $\mathcal{R}$-type and $\mathcal{C}$-type resonances involving large-n states of the hydrogen atom

We are going to take more specifically into account the fact that the environment seen by a system $\mathcal{S}$ depends on the state in which the system is. The hydrogen atom is a first example of a system about which one can answer the following general questions. When one considers atomic or molecular transitions between states whose spatial extension increases, does one see any decrease in the imaginary part of some of the associated resonances? In what conditions would the order of magnitude of the imaginary parts of the $\mathcal{R}$-type and $\mathcal{C}$-type resonances be comparable? To ask these questions is justified by the example of the charged harmonic oscillator studied in [20]. Let us recall the result. If physical parameters of the oscillator have such values that the spatial extension of the wave functions is large enough compared to the wavelength of the fundamental transition, then the $\mathcal{C}$-type resonance may become a (real) negative eigenvalue, therefore corresponding to a stable state. We want to set a calculus for extended states of the hydrogen atom, with a parameter measuring the ratio between the space extension and the transition's wavelength and calculate an example of a $\mathcal{C}$-type resonance. This study will also give us an opportunity to give a new example of a coupling function, in a case where no exterior constraint is applied on the atom-field system. In the cavity case, this constraint existed; it could suppress or enhance an atomic transition.

4.1 Setting of the calculus and introduction of non-dimensional variables

Let us consider a transition between two states $|1\rangle = |n_1, l_1, m_1\rangle$ and $|2\rangle = |n_2, l_2, m_2\rangle$ of the electron in the atom, accompanied by the emission of a photon. The space of possible photon states is assumed to be the space generated by states $|\gamma\rangle = |k, j, m, \lambda\rangle$, with variable energy $E = \hbar ck$, the angular momenta j, m and the polarization λ being fixed. The normalization is $\langle E, j, m, \lambda | E', j', m', \lambda'\rangle = E\delta(E-E')\delta_{j,j'}\delta_{m,m'}\delta_{\lambda,\lambda'}$. Taking $H_I = ie\hbar/(mc)\mathbf{A}.\nabla$ as the interaction Hamiltonian and assuming $j + j_1 + j_2$ to be for example even, we have (see for example [27])

$$g_I(k) := \langle 1|H_I|2,\gamma\rangle = C\big(A\phi_1(k) + B\phi_2(k)\big) \qquad (17)$$

where

$$\phi_1(k) = \int j_j(kr)R_1^*(r)\big(\frac{d}{dr}R_2(r)\big)rdr,$$
$$\phi_2(k) = \int j_j(kr)\big(\frac{d}{dr}R_1^*(r)\big)R_2(r)rdr. \qquad (18)$$

Constants A and B depend on the two considered states $|1\rangle$ and $|2\rangle$ and R_1, R_2 are the radial parts of their wave function. Let us neglect matrix elements of H which are not in the subspace generated by $|1\rangle$ and $|2,\gamma\rangle$. Let H' be the corresponding operator, acting in this subspace. The distance, which we call z, between eigenvalues or resonances of H' and the fundamental energy is one of the zeros of the following function

$$f(z) = z - \mathcal{E}_{n_1,n_2} - 2||g_I||^2 \int_0^\infty \frac{|g(k)|^2}{z-\hbar ck}\,\frac{dk}{k} \qquad (19)$$

or of its analytic continuation into the lower half-plane. $g(k)$ is $||g_I(k)||^{-1}g_I(k)$, with $||\theta|| = (2\int_0^\infty |\theta(k)|^2 dk/k)^{1/2}$ and $\mathcal{E}_{n_1,n_2}$ is the difference between the energies of states $|1\rangle$ and $|2\rangle$. The k^{-1} factor comes from the normalization of $|E, j, m, \lambda\rangle$. In preceding works, we studied the zeros of multivalued functions of the same form but with other g's.

Before we give indications on the form that g takes here in some particular transitions, let us show that the equivalent of parameter μ of Section 2.4 is now the ratio of the atomic transition wave-length to a length measuring the space extension of states $|1\rangle$ and $|2\rangle$. We have

$$R_1(r) = P_{n_1,l_1}(r/a_0)\exp(-r/(n_1a_0)),$$
$$R_2(r) = P_{n_2,l_2}(r/a_0)\exp(-r/(n_2a_0))$$

where P_{n_i,l_i} are polynomials and a_0 is the Bohr radius. Let us introduce $\overline{\rho}_{n_1,n_2} = \big((n_1a_0)^{-1} + (n_2a_0)^{-1}\big)^{-1}$, half the harmonic mean of the extensions n_1a_0 and n_2a_0 of $|1\rangle$ and $|2\rangle$. Let us set $y = 2\pi\overline{\rho}_{n_1,n_2}/\lambda_{\rm phot}$ and $G(y) = g(y/\overline{\rho}_{n_1,n_2})$. We have $||G|| = 1$, where $||G|| := \big(\int y^{-1}G(y)^2dy\big)^{1/2}$. Through also introducing the non dimensional variable $\zeta = z/\mathcal{E}_{n_1,n_2}$, $f(z)$ changes into $\mathcal{E}_{n_1,n_2}F(\zeta)$, with

$$F(\zeta) := \zeta - 1 - 2\kappa^2\int_0^\infty \frac{|G(y)|^2}{\zeta-\mu y}\frac{dy}{y}$$
$$= \zeta - 1 - 2\kappa^2\int_0^\infty \frac{|G_{(\mu)}(y)|^2}{\zeta - y}\frac{dy}{y} \qquad (20)$$

where

$$\kappa = \mathcal{E}_{n_1,n_2}^{-1}||g_I|| \quad\text{and}\quad \mu = \lambda_{n_1,n_2}/(2\pi\overline{\rho}_{n_1,n_2}) \qquad (20')$$

$G_{(\mu)}(y) = G(\mu^{-1}y)$ being obtained from G through the unitary dilation operator in $L^2(\mathbb{R}, dy/y)$. Remember that g_I and therefore κ depend on n_1, n_2, although it is not explicit in the notation. The study of the two type of resonances has been changed into the study of the zeros of the multivalued function F. Through comparing (20) with (8) we see that parameter μ here plays the same role as in Section 2.4: it dilates the coupling function. However, it is not exactly the same dilation.

4.2 Comparison between the$\mathcal{R}$-type and the $\mathcal{C}$-type resonances. Dependence with respect to the spatial extension of the naked states

If E_I is the atom's ionization energy, we have

$\mu = (n_1-n_2)^{-1}n_1n_2E_I^{-1}\hbar c/a_0 > E_I^{-1}\hbar c/a_0 \simeq 2/\alpha \simeq 274.$

We are going to show that the two zeros giving the $\mathcal{R}$-type and $\mathcal{C}$-type resonances are respectively close to 1 and $-i\mu$, if κ is small, which we will check in some examples in Section 4.3. We then get a qualitative answer to the two questions we asked at the beginning of Section 4. Firstly, provided κ does not change too much, one of the resonance does move towards the reals when the ratio of the mean extension of the states to the wavelength of the transition between them increases. Secondly, and this is eventually the important point in the present case, μ is large and, therefore, the $\mathcal{C}$-type resonances sit much farther from the real axis than the $\mathcal{R}$-type one and can be ignored. That there is a zero near 1 is clear. Let us show that there are zeros near $-i\mu$.

Function G depends on the states $|1\rangle$ and $|2\rangle$ but its poles do not depend on them. Let us show this if $j = 1$. Introducing $x := \overline{\rho}^{-1}r$, we get $\Phi_i(y) := \phi_i(y/\overline{\rho}) = \int_0^\infty j_1(yx)P_i(x)e^{-x}dx$, where P_i is a polynomial whose degree is at least 2 and at most $n_1 + n_2 - 1$. Setting $A_p(y) := \int_0^\infty j_1(yx)x^p e^{-x}dx = (-1)^{p+1}\big(x^{p+1}\frac{d^p}{dx^p}(x\mathrm{Arctg}(1/x))\big)_{x=1/y}$, we get, for $p \geq 2$,

$$A_p(y) = (-1)^{p+1}\frac{yQ_{p-2}(y)}{(1+y^2)^p} \tag{21}$$

where Q_{p-2} is a polynomial with degree at most $p-2$. As a consequence, $G(y)$ has the form $y\sum_{p\geq 2} a_p(1+y^2)^{-p}Q_{p-2}(y)$. Therefore, it has two poles and only one in the lower half-plane, at $y = -i$. Its order depends on the atomic transition which is considered. This implies that the analytic continuation of F into the lower half-plane has a pole at $\zeta = -\mu i$, since the integration contour in (20) is pinched between ζ/μ and $-i$, poles of the integrand. Its order is the same as that of G. It is this pole of F which is important for the $\mathcal{C}$-type resonances. (This was already the case in Section 2.4, since the position of the pole of f in (8′) was related to the width of g through the position of the pole of g.) Indeed, for small κ, the analytic continuation F_+ of F into the lower half-plane has several zeros $\zeta_{\mathcal{C},1}, \zeta_{\mathcal{C},2}, \cdots$ near this pole $-\mu i$. (Think of the function $\zeta - 1 - \kappa^2(\zeta - a)^{-n}$ which has n zeros near a.)

Let us note here that g derived from G is not of the form (7). But the existence of $\mathcal{C}$-type resonances is a general fact which does not depend on the particular form of g. In the present case, as the continuum is not narrow, there is no pertinent k_0.

Of course the exact position of the zeros of F associated with the $\mathcal{C}$-type resonances do depend on the exact form of G and not only on its pole. In particular the position also depends on the order of the pole: clearly, as the order increases, the zeros gets farther from the pole. In the numerical example we give in Section 4.3 below, the order of the pole is two. It is larger for other transitions. But on some examples we saw that increasing the order does not seem sufficient to move the $\mathcal{C}$-type resonances substantially closer to the real axis.

In conclusion, large-n states of the hydrogen atom do not give any other interesting resonances than the $\mathcal{R}$-type ones. Let us compare this result to the one we obtained for the extended system mentioned at the beginning of Section 4. We considered a quantum charged harmonic oscillator with charge 1, mass m and spring constant k_r. The level spacing is $\hbar\sqrt{k_r/m}$ and the exponential decrease of the wave functions is $\exp(-r^2/\delta^2)$, with $\delta = \hbar^{1/2}(k_r m)^{-1/4}$. The larger δ, the larger the extension. In a model in which this oscillator is coupled to the transverse electromagnetic field, we saw [20] that a $\mathcal{C}$-type resonance moves towards the reals when $2\pi\delta/\lambda = c^{-1}\hbar^{1/2}(k_r/m^3)^{1/4}$, the equivalent of $1/\mu$, increases. In particular, this resonance becomes even real negative if the ratio $2\pi\delta/\lambda$ becomes larger than $3\sqrt{2\pi}/\alpha$. In the hydrogen atom case, the ratio $2\pi\overline{\rho}/\lambda = \mu^{-1}$ remains smaller than $1/274$, and this implies that $\mathcal{C}$-type resonances always remain far from the reals. As regards the second question asked in the beginning of the section, it has to be noted that the distance of the $\mathcal{R}$-type resonance to the real axis is proportional to κ^2. Therefore, in the present study, since κ is small (see below), μ would have had to be much smaller than 1 in order that $\mathcal{R}$-type and $\mathcal{C}$-type resonances had comparable imaginary parts.

4.3 A numerical example

We might have calculated the $\mathcal{C}$-type resonances, in the two-level approximation, for transitions $n_1 \to n_2 = 1$, for which μ is close to its lower bound 274. However, in order to give an idea of the position of such resonances, it is sufficient to perform the calculation in the simpler case of the transition $|1\rangle = |2,1,0\rangle \to |2\rangle = |1,0,0\rangle$, for which μ is only twice the lower bound. The calculus is given in Appendix B. Here is the result.

The zeros of F are respectively $\zeta_{2,\mathcal{R}} \simeq 1 - 2\times 10^{-6} - 2\times 10^{-8}i$ on the one hand and $\zeta_{2,\mathcal{C},1} = 1.493 - 544i$, $\zeta_{2,\mathcal{C},2} = -1.474 - 551i$, $\zeta_{2,\mathcal{C},3} = 3.576 - 549i$, $\zeta_{2,\mathcal{C},4} = -3.595 - 546i$ on the other hand. The first zero gives the $\mathcal{R}$-type resonance: $z_{2,\mathcal{R}} = \mathcal{E}_{2,1}\zeta_{2,\mathcal{R}}$. Its imaginary part gives a life time $\tau_2 = 2\times 0.16\times 10^{-8}$ s, which has to be divided by 2 to take the other polarization into account. We thus recover the life time of the $2p$ state. The other zeros are $\mathcal{C}$-type resonances, very far from the real axis. The reason why there are four is that the coupling function has a double pole and is squared in the integrant in (20).

We have also calculated κ for the transitions between $|1\rangle = |n, n-1, 0\rangle$ and $|2\rangle = |n-1, n-2, 0\rangle$, with a photon in a state $(j, 0, +1)$. The result, given in Appendix B, shows that κ remains of the order of 0.02, when n varies between 10 and 50. Thus the non-dimensional coupling constant does not increase although $\mathcal{E}^{-1}_{n_1,n_2} \simeq n^3 E_I^{-1}$ gets large in (20′).

In order to get the exact position of the resonances, one should of course take other transitions into account (see [19]). But we do not see any reason why this should substantially displace $\mathcal{C}$-type resonances towards the real axis.

Regarding extended systems, we could think of hydrogenic excitons, whose mean radii may be as large as 2000 Å. But the associated Rydberg constant and Bohr radius are respectively $Ry^* = \epsilon_r^{-2}(m_{\mathrm{red}}/m_0)\ Ry$ and

$a_B^* = \epsilon_r(m_0/m_{\rm red})a_B$, $m_{\rm red}$ being the reduced mass of the electron-hole system, m_0 the electron's mass in the vacuum and ϵ_r the medium's relative permittivity ([8], formula (20a)); therefore, the ratio μ remains large.

5 Conclusion

The analysis in the complex energy plane of the resonances of a system $\mathcal{S}$ coupled to a continuum gives a precise mathematical description of mixed states which form in the interaction. Some of these mixed states may be assimilated to eigenstates of the Hamiltonian if the continuum is very narrow but, in general, they have a nonzero imaginary part, which may be large. When their imaginary part is so small that it can be considered to be zero, the corresponding eigenstates mix states of $\mathcal{S}$ with states of the continuum. It is these dressed states which are important in certain situations, for example in some spectroscopic measurements. When the imaginary part is not negligible, one has to deal with resonances, which we will still consider as associated to mixed (unstable) states. The description we get is more complete than the perturbative one based on the unperturbed states of $\mathcal{S}$.

These mixed states may be followed with respect to various parameters describing $\mathcal{S}$ or the coupling. When the parameter is the detuning, the description allows us to give a precise definition of the strong and weak coupling regimes. Data yield numerous examples of these mixed states when the continuum is narrow. Some are of the $\mathcal{R}$-type, others of the $\mathcal{C}$-type. Mixed states in the sense of the above paragraph also exist for the hydrogen atom coupled to the transverse electromagnetic field; but we saw that only the usual ones, corresponding to the unstable atomic levels, have a small imaginary part. They correspond to the resonances we called of $\mathcal{R}$-type. A condition for $\mathcal{C}$-type resonances to play a role for a system like the preceding atom is at least that its dimension be greater than the wavelengths of transitions between the system's eigenstates. This might be the case for non-localized electrons in large molecules. Let us also mention the case of strong interactions, in which transitions between states of the quark-antiquark system can have wave lengths of the same order as the extension of the states. Moreover, the coupling constant is not small. A calculation has been performed in [18].

Appendix A: A third resonance, if the pole of the coupling function is simple

We now study a zero of f_+ that we only mentioned at the beginning of Section 2.4.1, because we wanted to focus mainly on the weak/strong-coupling transition. We thus left aside resonances which had less importance, for the considered parameter values.

Let us recall that several resonances may be related to one another when several parameters are varied and that we must therefore be cautious in enumerating them. This is due to the fact that $f_+(\kappa, \mu, \delta, \zeta)$ is multivalued with respect to all variables.

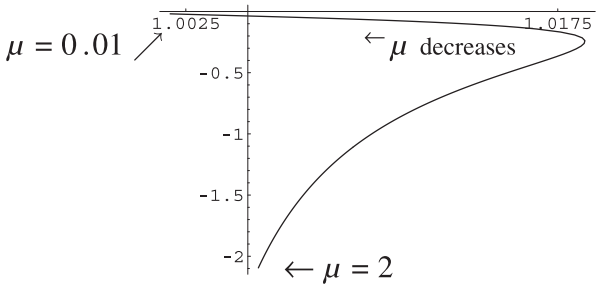

Fig. 10. A third resonance. Variation with respect to μ, for $\kappa = 0.1$ and $\delta = 0.25$.

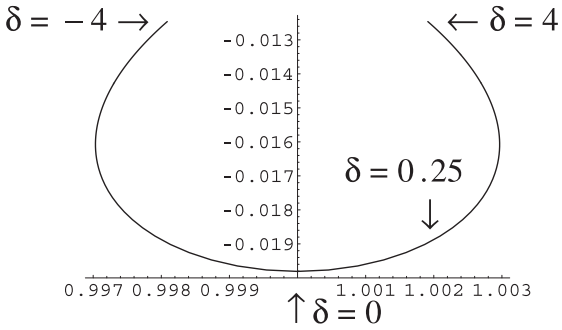

Fig. 11. A third resonance. Variation with respect to δ, for $\kappa = 0.1$ and $\mu = 0.01$.

When κ and δ are fixed, for example as in Figure 1, and μ is the only parameter to vary, not all zeros of $f_+(\kappa, \mu, \delta, .)$ are described by the curves in Figure 1. There exists another zero which we now describe. We denote it by $\zeta_u(\mu)$, a function defined from its values for large μ. More precisely, for $\mu = 2$, $f_+(\kappa, \mu, \delta, .)$ has a zero at $\zeta_u = 1.005 - 2.095i$, which differs from $\zeta_{w,ph}(2)$ which is $0.993 - 1.895i$. Following the displacement of this new resonance when μ decreases, we obtain $\zeta_u(\mu)$, represented by the curve in Figure 10. When μ tends to 0, ζ_u tends to 1, the energy of the decoupled photon; one can check that this remains true for other values of κ. When μ increases, ζ_u seems to be asymptotic to $1 - i\mathbb{R}^+$, behaving like $1 - i\mu$. Let us give the type of $\zeta_u(2)$: it can be seen that the resonance sitting at $\zeta_u(2)$ tends to $1 - 2i$ when κ goes to 0. Like $\zeta_{w,ph}(2)$, $\zeta_u(2)$ is therefore a $\mathcal{C}$-type resonance.

When δ is the parameter which is varied, κ and μ now being fixed, a third curve has also to be added to the two curves in Figure 4. The curve generated from the point of Figure 10 at $\mu = 0.01$ ($\zeta = 1.0019 - 0.019i$) is shown in Figure 11.

The limits when δ goes to $\pm\infty$ can be checked to be again equal to $1 - i\mu$. Collecting the results of Figures 4 (or 5) and 11, we see that there are two resonances tending to $1 - i\mu$, and one behaving as $1 + \delta$, when $\delta \to +\infty$. The same for $\delta \to -\infty$.

That there are actually three resonances for each value of the parameters can be seen as follows. If κ is small, there is obviously a zero of f_+ near $1 + \delta$, the energy

(in $\hbar c k_0$ units) of the unperturbed excited state of $\mathcal{S}$. For mathematical reasons, there is also a resonance near $1-i\mu$ (the enlarged energy of the photon), but the point is that the zero of f_+ is double, which yields two resonances and not one. Indeed, deforming the integration contour in (8′), we can show that for $\Im\zeta < 0$,

$$f_+(\kappa,\mu,\delta,\zeta) = f(\kappa,\mu,\delta,\zeta) - 4i\kappa^2\mu^3\left(\frac{1}{(\mu^2+(\zeta+1)^2)^2} - \frac{1}{(\mu^2+(\zeta-1)^2)^2}\right).$$

For $\Im\zeta < -\epsilon$ et $\Re\zeta > 0$, we then have, for fixed μ and δ,

$$f_+(\kappa,\mu,\delta,\zeta) = \zeta - 1 - \delta - \frac{c_2\kappa^2}{(\zeta-(1-i\mu))^2} - \frac{c_1\kappa^2}{\zeta-(1-i\mu)} + o(\kappa^2).$$

Therefore, for κ small, one sees that, besides the zero near $1+\delta$, f_+ has indeed two zeros near $\zeta = 1-i\mu$, the limit of which is $1-i\mu$ when κ goes to 0.

The three resonances for small κ are related to the three curves of Figures 1 and 10 in the following way. Let us fix $\mu = 0.01$ and $\delta = 0.25$, to be concrete, and start following the three resonances as κ increases from very small values up to 0.1. The three resonances end up at three points each one sitting on one of the three curves in Figures 1 and 10.

Physically, each resonance contributes to the time-dependence of $\langle 1|e^{-itH/\hbar}|1\rangle$ through a contour integral in the energy complex-plane, (see Sect. A$_{III}$.4 of Ref. [24]). We note that the contribution of the resonance of Figure 11 is negligible, in particular for $\delta = 0$. Indeed, for every δ, its imaginary part is greater than -0.019, which makes its contribution to $\langle 1|e^{-itH/\hbar}|1\rangle$ of the order of $Ce^{-0.02(ck_0)t}$, a quantity rapidly much smaller than the contribution of the two other resonances whose imaginary parts are of the order of 10^{-4}. (The latter imaginary parts yield a slight damping of the Rabi oscillation between states $|1,0\rangle$ and $|0,1\rangle$.) In problems in which neither the coupling constant nor the continuum's width are small, the three resonances are to be considered. Let us mention again that the number of $\mathcal{C}$-type resonances is greater than three if the pole of the coupling function is not simple. This is illustrated in the hydrogen-atom case.

Appendix B: Calculation of $\mathcal{C}$-type resonances for the hydrogen atom

The radial parts of the wave functions of states $|n,n-1,0\rangle$ and $|n-1,n-2,0\rangle$ are

$$R_1(r) = K_n a_0^{-3/2} e^{-r/(na_0)}(r/a_0)^{n-1},$$

$$R_2(r) = K_{n-1} a_0^{-3/2} e^{-r/((n-1)a_0}(r/a_0)^{n-2}$$

where $K_n = (2/n)^{n+1/2}((2n)!)^{-1/2}$ normalizes the wave function. Let the subscript n index all quantities related to the transition $|n,n-1,0\rangle \to |n-1,n-2,0\rangle$, with emission of a photon ($j = 1,0,+1$). The function $g_{I,n}(k) := \langle 1|H_I|2,\gamma\rangle$ corresponding to this transition is (see for example [27])

$$g_{I,n}(y/\overline{\rho}) = -i\frac{\sqrt{3}}{2\sqrt{\pi}}\alpha^{1/2}(e^2/\overline{\rho}_n)(\overline{\rho}_n/a_0)^{2n} D_n\varphi_n(y)$$

where

$$D_n = \frac{K_n K_{n-1}}{n\sqrt{(2n-1)(2n-3)}},$$

$$\varphi_n(y) := y\frac{\alpha_n Q_{2n-4}(y) + \beta_n(1+y^2)Q_{2n-5}(y)}{(1+y^2)^{2n-2}}$$

with

$$\alpha_n = 2n^2 - 3n + 2, \quad \beta_n = (2n-1)^2(n-2)$$

Q having been defined by (21). G, μ and κ in (20) are then, for the considered transition,

$$G_n(y) = ||\varphi_n||^{-1}\varphi_n(y), \qquad \mu_n = n(n-1)E_I^{-1}\hbar c/a_0$$

and

$$\kappa_n = \frac{(3\alpha)^{1/2}}{2\sqrt{\pi}}(e^2/\overline{\rho}_n)(\overline{\rho}_n/a_0)^{2n} D_n\mathcal{E}^{-1}_{n,n-1}||\varphi_n|| = \frac{(3\alpha)^{1/2}}{2\sqrt{\pi}}\frac{e^2/a_0}{E_I}\frac{(n(n-1))^{2n+1}}{(2n-1)^{2n}}D_n||\varphi_n||.$$

Through using $e^2/a_0 \simeq 2E_I$, we get $\kappa_n \simeq \sqrt{3/\pi}\alpha^{1/2}(n(n-1))^{2n+1}(2n-1)^{-2n}D_n||\varphi_n||$. A computer gives

$$\kappa_2 = 0.018, \quad \kappa_{10} = 0.022, \quad \kappa_{50} = 0.028$$

and, for $n = 2$,

$$\mu_2 \simeq 548 \quad \text{and} \quad G_2(y) = -\sqrt{3}\frac{y}{(1+y^2)^2}.$$

The five zeros of F are then respectively $\zeta_{2,\mathcal{R}} \simeq 1 - 2\times 10^{-6} - 2\times 10^{-8}i$ and $\zeta_{2,\mathcal{C},1} = 1.493 - 544i$, $\zeta_{2,\mathcal{C},2} = -1.474 - 551i$, $\zeta_{2,\mathcal{C},3} = 3.576 - 549i$, $\zeta_{2,\mathcal{C},4} = -3.595 - 546i$.

References

1. C. Cohen-Tannoudji, B. Diu, F. Laloë, *Mécanique Quantique* (Hermann, Paris, 1973)
2. T. Inoshita, H. Sakaki, Phys. Rev. B **56**, R4355 (1997)
3. M. Reed, Sci. Am. **268**, 98 (1993)
4. O. Verzelen, R. Ferreira, G. Bastard, Phys. Rev. B **62**, R4809 (2000)
5. O. Verzelen, R. Ferreira, G. Bastard, Phys. Rev. Lett. **88**, 146803 (2002)

6. S. Hameau, Y. Guldner, O. Verzelen, R. Ferreira, G. Bastard, J. Zeman, A. Lemaître, J.M. Gérard, Phys. Rev. Lett. **83**, 4152 (1999)
7. F. Boeuf, R. André, R. Romestain, Le Si Dang, E. Péronne, J.F. Lampin, D. Hulin, A. Alexandrou, Phys. Rev. B **62**, R2279 (2000)
8. C. Weisbuch, B. Vinter, *Quantum Semiconductor Structures* (Academic Press, San Diego, 1991)
9. B. Sermage, S. Long, I. Abram, J.Y. Marzin, J. Bloch, R. Planel, V. Thierry-Mieg, Phys. Rev. B **53**, 16516 (1996)
10. Y. Yamamoto, F. Tassone, H. Cao, *Semiconductor Cavity Quantum Electrodynamics* (Springer, Berlin, 2000)
11. P. Senellart, Ann. Phys. Fr. **28**(4) (2003)
12. J. Tignon, P. Voisin, C. Delalande, M. Voos, R. Houdré, U. Oesterle, R.P. Stanley, Phys. Rev. Lett. **74**, 3967 (1995)
13. S. Haroche, *Rydberg atoms and radiation in a resonant cavioty*, in Les Houches, XXXVIII (North Holland, Amsterdam, 1984)
14. S. Haroche, *Cavity Quantum Electrodynamics*, in Les Houches, LIII (North Holland, 1992)
15. S. Haroche, J.M. Raimond, Sci. Am. **268**(4), 26 (1993)
16. *Cavity Quantum Electrodynamics*, edited by P. Berman (Academic Press, 1994)
17. J.M. Raimond, M. Brune, S. Haroche, Rev. Mod. Phys. **73**, 565 (2001)
18. C. Billionnet, Int. J. Mod. Phys. **19**, 2643 (2004)
19. C. Billionnet, J. Math. Phys. **46**, 072101 (2005)
20. C. Billionnet, J. Phys. A **34**, 7757 (2001)
21. C. Billionnet, J. Phys. A **35**, 2649 (2002)
22. V. Savona, L.C. Andreani, P. Schwendimann, A. Quattropani, Solid Stat. Comm. **93**, 733 (1995)
23. A. Arai, J. Math. Anal. Appl. **140**, 270 (1989)
24. C. Cohen-Tannoudji, J. Dupont-Roc, G. Grynberg, *Processus d'interaction entre photons et atomes* (CNRS, Paris, 1988), (Engl. transl.: Wiley, New York, 1992)
25. C. Weisbuch, M. Nishioka, A. Ishikawa, Y. Arakawa, Phys. Rev. Lett. **69**, 3314 (1992)
26. J. Callaway, *Quantum Theory of the Solid State* (Academic Press, New York, 1974)
27. H.E. Moses, Phys. Rev. A **8**, 1710 (1973)